**BUKU PROFIL PENYELIDIKAN SKIM GERAN PENYELIDIKAN FUNDAMENTAL (FRGS)**

---

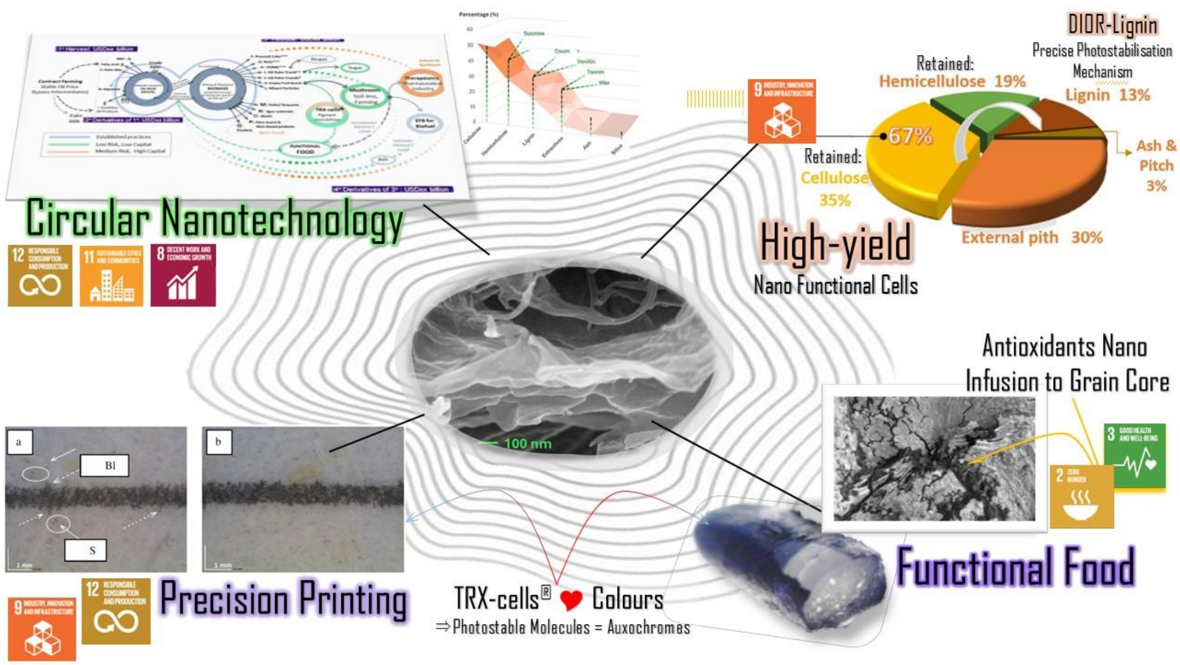


# MECHANISMS OF MICROFIBRE DECONSTRUCTION FOR ABSOLUTE YIELD OF NANO-SCALE FUNCTIONAL MATERIALS


Arniza Ghazali
Mohd Rafatullah Lari
Ahmad Naim Ahmad Yahaya
Melati Khairuddean
Md Sohrab Hossain

Universiti Sains Malaysia
School of Industrial Technology

arniza@usm.my


**Pure and Applied Science**

## ABSTRACT

The end-of-life of the non-recyclable EFB alkaline peroxide fibres was extendable when the mechanisms of harvesting the nano-structured cells were elucidated. Through 17000 kWh/mt mechanical shearing impact, cells of 5 nm to 100 nm thickness peeled. The energy intensiveness can be resolved by supercritical fluid extraction of radical treated EFB. The cells with 60% crystallinity blended cellulose, auxochromes, xylan and nano-minerals, accounted for the 24% enhanced softness. Registered as 'TRX-cells®, the cells portray affinity for colours, enabling precision printing when coated on commercial A4 paper and delivery of plant pigments to the grain core. The cells cascading mechanism fulfills a closed-loop process, demonstrating the actualisable circular nano technology in EFB utilisation, harmonising people-nature-technology coexistence through an accentuated profit for sustainability.

## 1. INTRODUCTION

EFB, the acronym for Oil Palm Empty Fruit Bunch, is the commodity from the mill rather than the plantation. Despite its abundance and value, EFB is still underutilised, but its vascular bundles are availed in the market as 'dried long fibre'. Due to its scattered market, their use as plant potting substrate is popular but the application does not efficiently maximise the inorganics as well as the predominant organic portion of the biomass, but the natural high-emission degradation. Analogous to straw whitening in hat making, dioxydanyl radicals (DIOR) engendering lignin conversion to auxochromic molecules [1-6] was the driver for the two-in-one cellulose extraction and photo-stabilising processes. Eliminating the need for a separate bleach plant is the instantaneous path to capital-saving [5, 6]. The dearomatisation concept allows the system to offer high-yield and high-brightness output, fulfilling the resource efficiency criteria posited by Pena *et al*. [7].

Cumulative research on alkaline peroxide pulping of EFB proved the possibility of a high-strength fibre web that was only imperfect for recycling. The drawback is grievous considering the existing 680,000 trees-equivalent local paper wastes [8] and those occupying 10-40% of worldwide landfills. Thus, attempts to divert such non-recyclable fibres [9] and transform them into a value-added commodity is a saviour move towards a *closed but extendable, and intensifying loops strategy* [10] for circularity. In this study, we transformed the non-recyclable fibres to a higher-value cell mass for microscopic, spectroscopic, and crystallographic analyses. The understanding deepened by correlating the data with the functional properties imparted by the cell's rice and paper coatings performances. The findings allowed warrant assessment circularity fit within the oil palm residue (OPR) circularity model.

Downsizing the DIOR-treated EFB via Andrits refining system and half the maximum PFI milling [11], the fibre web's resistance to the pulling forces revealed an extraordinary tensile index (54 mN/g [12] arising from the synergy between sophisticated molecular scale and physical interlocking, interdiffusion, electrostatic, capillary bridge, micro-compression, hydrogen bonding, van der Waals forces as well as the C-O:::H related hydrogen bonding [13, 14].

To elucidate the underlying mechanisms, the deconstruction effects and the cell morphological transition with the cascading impact were examined. A creative thought process is required to imagine the correct mounting technique and the processes needed to reach the target answer to the research question. The section that follows narrates the old and new techniques of cell analysis ranging from classical to spectroscopy and advanced electron microscopy. The research attempted to answer critical mechanistic questions and concluded that the mechanical actions, whether from solid punches or gaseous bombardments, worked in synergy with the preceding chemical reaction. DIOR-EFB, the backbone for EFB fibre deconstruction, therefore, has to be efficient. Additional steps are synonymous with additional capital and are excluded from the write-up. Understanding the reactivity and lability of components to DIOR is the key to mechanistic elucidation. Thus, this chapter presents the impact the DIOR-treated experienced, leading to TRX-cells® alongside the application of new formulae and metrics in materials characterisation.

## RESEARCH METHODOLOGY

### Mechanism of DIOR-Initiated Fibre Deconstruction

EFB microfibre deconstruction was studied by delving into the properties of the cascaded cells. Under conditions that support the dioxydanal radicals (DIOR) formation, the vibrant bubbling and whitening of the biomass in the reaction chamber after several minutes of darkening were the unique indicators of DIOR pre-treatment occurring at the desired level. A custom design setup was adopted to ensure constant contact between the biomass and the DIOR solution despite a 10-to-1 liquor-to-biomass ratio. For a brightened fibrous mass with Kappa Number above 90%, a high-yield figure is expected and this means that the DIOR reaction had modified the micro-molecular lignin into photo-stable fragments.

**Cell Softness:** Webs of cells derived from 0 to 1700 kWh/t each milling energy were subject to underwent tear resistance and optical tests per TAPPI (1997) Test Method T414 om-98 and T425 [15,16], respectively. The study established a method for measuring cell softness from the tear resistance profile depicted in formula 1:

Cell Softness Enhancement (%) = (Initial Tear Index)/Ultimate Tear Index) x100 …[1]

**Cell Microscopy:** Nano-scale masses were first confirmed by the cloudy appearance detected under the light microscope. From this checkpoint, samples were prepared appropriately to detect the detailed view of the nanoscale call mass. The 3D appearance of delaminated cells was captured using Leo Supra 50VP Carl Zeiss Scanning Electron Microscope (SEM). The standard R200 or 'accepts' amongst the pulp mass is denoted microfibres or "$\mu$-fibre" and the PFI-milled cells registered with "TRX-cells®" trademark are also referenced as "nano cells" and "TRX", interchangeably.

The advanced microscopy at the Science and Engineering Research Centre, SERC, Universiti Sains Malaysia's Engineering Campus were chosen as the analysis hub due to their familiarity with handling the samples from the project. High-resolution Transmission Electron Microscopy (HRTEM, FEI TECNAI G2) of the obtained cells mounted on copper and lacey carbon grids enhanced the qualitative and semi-quantitative elemental mapping through the Oxford X-MaxN 80 $mm^2$ with INCA software. A prolonged electron bombardment triggering rupture of the non-conductive hydrocarbon cells was the mark for differentiating the cells from the lacey carbon. Extra High-resolution Field Emission Scanning Electron Microscopy (XHR-FESEM) was also accessed when differentiation between atomic level tones was required.

**Relative Crystallinity**

**X-Ray Diffraction:** While X-ray Diffraction spectroscopy is well-known for accurate estimation of crystallinity of inorganic samples, FTIR has in recent days established a better measure of crystallinity or the organic cell mass. This study opted for both techniques to also prove dearomatisation of the ligno-components. X-ray Diffraction (XRD), designed for clearcut crystallography of inorganic crystal lattices, was employed to benchmark the overall crystallinity transition of the feedstock to nano cells. Crystallinity values commonly derived from XRD were used to probe the raw changes of the cell mass while specific changes in the organic functional groups related to DIOR reaction with EFB were spotted in Fourier Transform Infrared (FTIR) relative crystallinity. The X-ray Diffractograms of the raw material (Biomass Feedstock), microfibre ($\mu$-fibre) and the nano cells or TRX-cells® were compared. XRD was performed on a goniometer using CuKα anode radiation generated at 40 kV and 35 mA. The CuKα radiation consists of Kα1 (0.15406 nm), Kα2 (0.15443 nm) and the subtracted Kβ2 (0.13923 nm) component. The 0.5-1 mm slits were fixed for a 320 mm goniometer working radius to handle signals from approximately 0.5-1 g dried samples mounted onto a quartz stub. Samples' crystallinity indices (CI) were calculated from the height ratio between the intensity of the crystalline peak ($I_{200}$ - $I_{AM}$) and total intensity ($I_{200}$) after correction for the background signal. The crystallinity index was derived from equation 1, deemed the most robust measure for crystallinity derivation proposed by Park and team (2010) [17].

$$\text{Crystallinity Index, CI} = (I_{200} - I_{AM}) / (I_{200}) \text{ ......[2]}$$

Fourier Transform Infrared (FTIR) spectra of the soft matter possessing weaker intercomponent bonds (cf. inorganic crystal latices) typical of cellulosic samples (EFB feedstock, dioxydanyl-reacted refined EFB ('μ-fibres') and PFI-milled mass) were acquired using the Perkin Elmer's Frontier FT-IR/NIR interfaced with MIR-TGS detector and UATR accessories. A total of 16 cumulative scans were taken, at a resolution of 8 $cm^{-1}$, in the default frequency range of 4000-650 $cm^{-1}$. Similar to the work of Ciolacu and team [18], crystallinity values were then derived from the ratio of the absorbance signals (Abs) corresponding to bands sensitive to crystallinity changes at 2900 $cm^{-1}$ with the relatively unsusceptible band at 1372 $cm^{-1}$ as indicated in Equation 3.

$$\text{Crystallinity} = Abs_{2900}/Abs_{1372} \text{x} 100 \text{ ........... [3]}$$

**Spectroscopic Analysis:** The functional group transformation was also tracked via Perkin Elmer's Frontier FT-IR/NIR interfaced with the MIR-TGS detector and UATR accessories. The nano cell isolates were dried and analysed in triplicate. Dearomatisation, referencing the cleavage of the benzene ring due to electron localisation in the presence of dioxydanyl radical, was detected by examining the 1000-1500 $cm^{-1}$ region.

**Circularity Metrics**

As the circular bioeconomy principles emerged and is becoming dominantly trending, the study establishes a simplified method for determining the circularity fit specific to EFB utilization. The estimation takes selected parameters in Table 1 into account and the aim was to decide on the products promoting circularity for inclusion in the circular nanotechnology diagram.

**Table 1**: Thought Process Behind Circularity Metrics

| PARAMETER | MAXIMUM WEIGHT | DEFEATING FACTOR |
|---|---|---|
| UN SDG | Aligned to global move | Baseless 'sustainability', 'economic', 'eco-friendly' claims. |
| Water Consumption | Looping is a plus. | Water intensiveness. |
| Market Deliverability | Solution to pressing issues. | Impractically complex. |
| Industrial Symbiosis | Promotion of equity. | Suppressive. |
| Carbon Cycle | C-Sink or C-sequestration. | Carbon loss and emission. |

While proven market viability (high demand & less adverse repercussions) carries the highest weight, a track record of proven commercial failure and bankruptcy is lightest in in the weight scale. The Circularity Fit discussed throughout the report refers to the evaluation in Table 2.

**Table 2:** Circularity Fit Assessment for Oil Palm Biomass
Reproduced from Reproduced from https://doi.org/10.1016/j.heliyon.2024.e30824.

| BOTANICAL PARTS / COMPONENTS AS PRODUCTS | MARKET DELIVERA -BILITY | INDUSTRIAL SYMBIOSIS PRACTICALITY | PRODUCT USABILITY UP TO CARBON FIXATION | CIRCULAR WATER MANAGEMENT | UN SDG RELEVANCE | OVERALL CIRCULARITY FIT |
|---|---|---|---|---|---|---|
| (A) **EFB** [2, 8, 9] | ✓✓✓✓✓ | ✓✓✓✓✓ | ✓✓✓✓✓ | ✓✓✓✓✓ | SDG12, 13 | ☑ |
| (B) **OPF** [10] | ✓ | N/A | ✓✓✓✓✓ | N/A | SDG 11, 12 | ☑ |
| (C) **OPT** [11-13] | ✓✓✓✓✓ | ✓✓✓✓✓ | ✓✓✓✓✓ | ✓✓✓✓✓ | SDG 12 | ☑ |
| (D) **POME** [14] | ✓ | N/A | N/A | N/A | SDG 12 | ☑ |
| Derivatives of A, B & C: | | | | | | |
| (E) **ASH** [15] | ✓✓✓✓✓ | ✓✓✓✓✓ | ✓✓✓✓✓ | N/A | SDG 12 | ☑ |
| (F) **FINES** [16, 17] | ✓ | ✓ | ✓ | N/A | SDG 2, 6, 12 | |
| (G) **WAX / LUBRICANT** [18] | ✓✓✓ | ✓✓✓✓✓ | ✓✓✓✓✓ | ✓✓✓✓✓ | SDG 12 | ☑ |
| (H) **LIGNIN** [18] | ✓✓✓✓✓ | ✓✓✓✓✓ | ✓✓✓✓✓ | ✓✓✓✓✓ | SDG 12 | ☑ |
| (I) **SUGAR** [13] | ✓✓✓✓✓ | ✓✓✓✓✓ | ✓✓✓✓✓ | ✓✓✓✓✓ | SDG 2, 12 | ☑ |
| (J) **NANOCELLULOSE** | ✓ | ✓ | ✓✓✓✓✓ | ✓✓✓✓✓ | ⊥ | ⊥ |
| (K) **NANO CELLS** [19, 20] | ✓✓ | ✓✓ | ✓✓✓✓✓ | ✓✓✓✓✓ | SDG 2, 12 | ☑ |
| (L) **NANO MINERALS** | ✓✓✓✓✓ | ✓✓✓✓✓ | ✓✓✓✓✓ | ✓✓✓✓✓ | SDG 12, 13 | ☑ |
| (M) **ADSORBENTS** [21, 22] | ✓✓✓✓✓ | ✓✓✓✓✓ | ✓✓✓✓✓ | ✓✓✓✓✓ | SDG 6, 12, | ☑ |

✓✓✓✓✓ ≡ Proven market of various scales / SMEs / Cottage Industry
✓✓✓ ≡ Technology in place and applied commercially on other biomass
✓✓ ≡ System's byproducts underwent studies for rerouting to specific use. Prototyping is in progress.
✓ ≡ Intensively researched by related industry.
⊥ ≡ Commercial scale chemical pulp production from EFB ceased for reasons discussed elsewhere [23]. Chemical pulp is the feedstock for most nanocellulose production.
☑ ≡ Fit for inclusion in the circularity model (Figure 10).
EFB ≡ Empty Fruit Bunch
OPF ≡ Oil Palm Fronds
OPT ≡ Oil Palm Trunk
POME ≡ Palm Oil Mill Effluent
UN SDG ≡ United Nation's Sustainable Development Goal [24]
NB: Initiatives enabling food security is classified under Zero Hunger, SDG 2.

## 2. LITERATURE REVIEW

The alkaline peroxide lignin modification has been an established reaction since the first industrial revolution. It only came to the fibre extraction industry as many died of cancer due to the dioxin type of byproduct released in chlorine bleaching of papermaking fibres.

The skilled technique of handling the precursor generated the dioxydanyl radicals (DIOR) leading to Reaction 1.

$$H_2O_2 + OH^- \longrightarrow OOH^\cdot + H_2O$$

Dioxydanyl radicals (DIOR)

**…Reaction 1**

At the right pH, these radicals initiate electron localisation. Cleavage of the aromatic ring into an aliphatic moiety released the ‘radical-altered lignin’ or “RADIAL”. It is this ‘dearomatisation’ stage in Reaction 2 that allows effective fibrillation of vascular bundles to fibres.

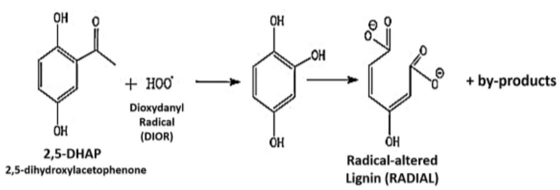


**…Reaction 2**

## 3. FINDINGS

**Mechanism of Nano Cells Generation:** Web durability is the picture of the cells domiciling the web. The tear resistance profile (Fig. 1a) provided a wealth of clues for the nature of crack propagation. Data from this research revealed a trend mimicking the behaviour of soft matter [19] contrasting the fracture mechanics theories [20]. Morries [21] attributed the sum of the impeded tear strength of the individual constituents added up to the resultant profile. Specific to the studied cells constituting the web, the negative slope correlates with the degree of the accentuated binding materials. While the first down-trend phase is associated with the liberation of binder that causes splitting of fibre bundles, the more vivid phase of tear obstruction correlates with the extent of fibrous mass redistribution shown as the circled cell mass (CM) in Fig. 1b iii-v, which possesses lower individual strength than their intact fibrils (IF).

Tear, which occurs by propagation of cracks from the strain-concentrate initiation point, involves obstruction along the sacrificial bond [20]. In the case of the generated cells, the tearing occurred at the CM-IF interface (Fig. 1b), suggesting a weakening of the web as the thin cells formed the fixation points on the intact fibril in the cell web. As beating intensified, the redistributed mass of binding materials consisting of both the DIOR-reacted or the dearomatised ligno-fragment and the DIOR-resistant non-cellulosic became the interlayering binder in between fibrils. The CM-IF resulted in webs of declining tear indices similar to the profile uncovered portrayed by softwood fibres [22]. As the cell mass compacted into a 60-gsm web, the inter-fibre micropores were filled up with the soft elements, restricting constituent mobility or ability to slide, which Eltahan [23] identified as a factor for the declining tear strength.

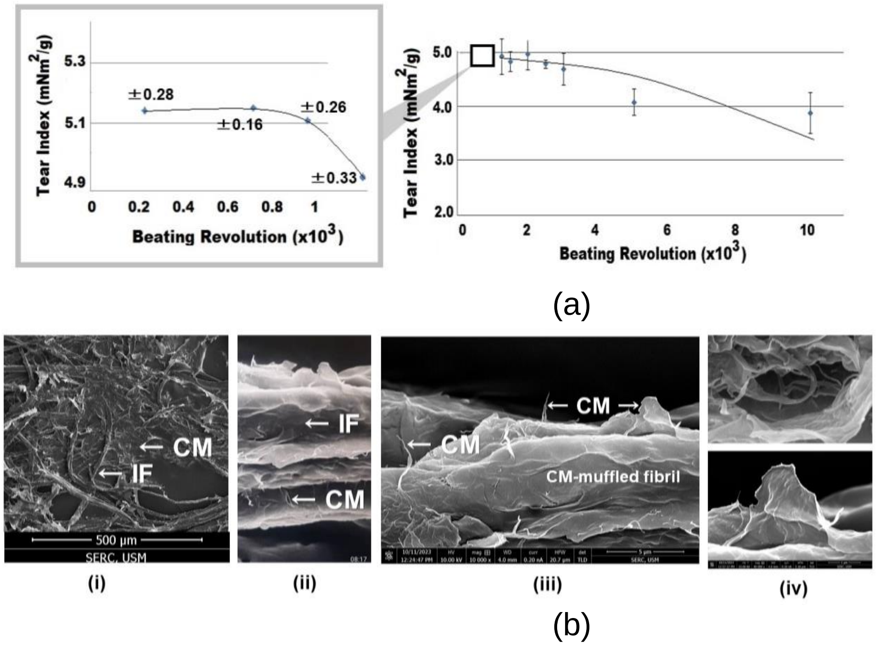


**Figure 1:** Transition of cell softness is captured in (a) tear profile, triggering curiosity to perform (b) a close-up look at the cells. Reproduced from https://doi.org/10.1016/j.heliyon.2024.e30824

The extremely thin cells in Figure 1b-iv and the unique mechanics of soft materials can be maximized to reduce analysis costs, especially at the industrial production line. A little scientific tapping into the area would add efficiency to the existing quality control measures. Specific to the materials in focus, the cells must have contained DIOR-resistant elements like hemicellulose [24-26], pectin, polyphenolic material, structural glycoproteins, and small quantities of proteins contributing to the 26% softness enhancement.

Given the ligno-components' susceptibility to DIOR, the observed cell thinning (that favoured web tensile over tear resistance), also reflects the extent of DIOR penetration. Overall, intra-fibre bond breaking, fibre cutting (segmentation) and external fibrillation, which led to cell wall peeling or 'delamination' were all spoken by the micrograph in Figure 2.

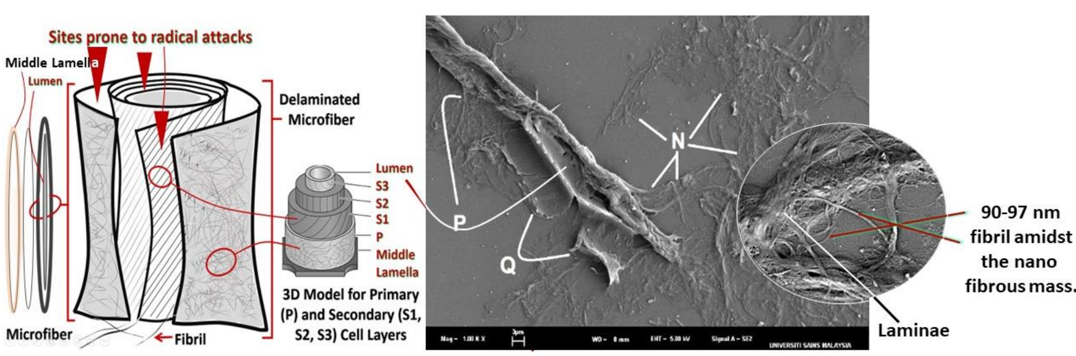


**Figure 2:** Delaminated cell walls reflecting the extent of DIOR-EFB reaction and permeation. Reproduced from https://doi.org/10.1016/j.heliyon.2024.e30824.

**Quantitative Accounts of Soft Transition:** The highest semi-crystallinity is attributable to the ordered cellulose and the ordered dearomatised components in the intact alkaline peroxide fibres. TRX-cells®, consisting of the unravelled DIOR-resistant hemicelluloses, fibrils, auxochromic molecules and nano-minerals gave rise to a 7-14% drop in crystallinity. Signals associated with the preferred (110) and (200) crystal lattices [25, 26] show crystallinity reduction of the milled nano-scale cells (denoted TRX-cells®) attributable to the attenuated intra- and intermolecular hydrogen bond of the lignocellulosic composite. The apparent enlargement in the FTIR signal (3300 $cm^{-1}$) in Figure 3 is consistent with the collective increase in the hydroxyl groups with RADIAL (Reaction 2).

| **FTIR Band** A ≡ Absorbance (a.u.); T ≡ Transmittance (%) | **µ-fibre (µf)** | **TRX** | **EFB** | **% Difference EFB-µf** | **% Difference µf-TRX** | **% Difference EFB-TRX** | **% Change EFB-µf** | **% Change µf-TRX** | **% Change EFB-TRX** |
|---|---|---|---|---|---|---|---|---|---|
| T (%) | 90.93 | 94.1 | 98.55 | | | | | | |
| A (2900 $cm^{-1}$) | 0.048 | 0.027 | 0.007 | | | | | | |
| T (%) | 87.2 | 91.48 | 97.3 | | | | | | |
| A (1372 $cm^{-1}$) | 0.066 | 0.04 | 0.013 | | | | | | |
| **Crystallinity (%)** (FTIR) | **73** | **68** | **54** | **30** | **7** | **+23** | **26** | **-7** | **+26** |
| **Crystallinity (%)** (XRD) | 64 | 55 | 37 | **15** | **15** | **+39** | **16** | **-14** | **+49** |
| **Average** | 68.5 | 61.5 | 45.5 | **15** | **11** | **31** | **21** | **10.5** | **37.5** |

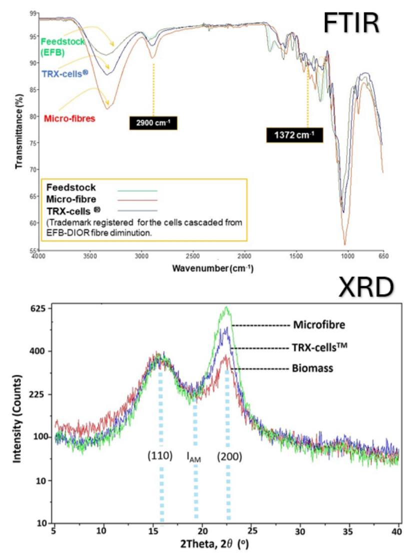


**Figure 3:** Consistent trend in crystallinity from XRD and FTIR. Reproduced from https://doi.org/10.1016/j.heliyon.2024.e30824.

The redistributed recalcitrant cells, including the non-cellulosic mass, led to an overall crystallinity reduction from a 64-73% range to 55-68%. Delamination was elucidated as occurring at the weakened middle lamella following the detection of nano calcium. Calcium pectinate's role in mediating ionic interactions linking the pectins in the middle lamella to the pectins in the primary cell walls is an important illumination. The evidence also provides a matching account for cell thinning in line with the middle lamella's reported 50 nm thickness [27]. High-resolution TEM testified the cell's thickness ranging from 5 – 100 nm (Fig. 4), validating also the presence of fibril*s-embedded hemicellulose* [27]. As much as middle lamella prevents living cells from sliding away from each other, it also limits the liberation of the fibril, defying the formation of nanorods.

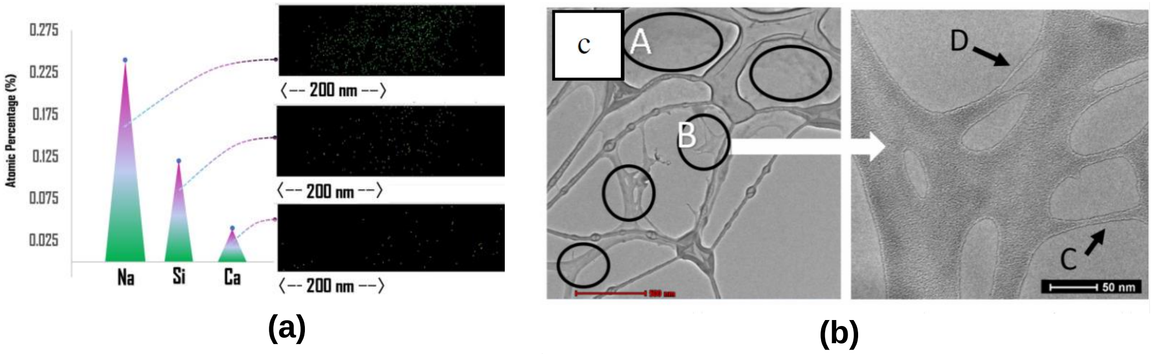


**Figure 4:** HRTEM analysis of TRX-cells®. Uncovering (a) nanoscale inorganics in the elemental mapping of the cells in (b) theoretically matched to the middle lamella. Reproduced from articles at https://doi.org/10.1016/j.heliyon.2024.e30824 and https://doi.org/10.35812/cellulosechemtechnol.2021.55.92.

In essence, alongside the cascaded TRX-cells® are the nanometre scale bio-binder that co-exists with bio-inorganics. The nano-scale components constituted in the TRX-cells® functionalised its coating for precision printing (Figure 5) and antioxidant-loaded grain coatings (Figure 6).

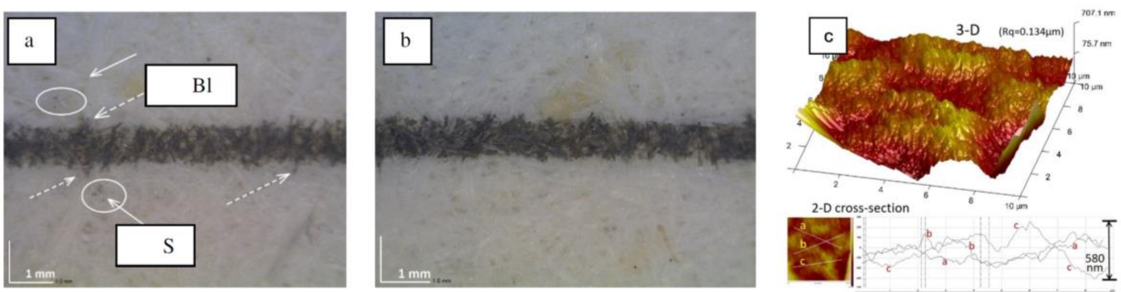


**Figure 5**: Inkjet ink distribution on A4 paper (a) without TRX-cells® and (b) with TRX-cells® through ink sipping and floating mechanisms via the (c) nano canals created with TRAX-cell® atop the A4. Reproduced from https://doi.org/10.35812/cellulosechemtechnol.2021.55.92.

Pigment-TRX-cells® affinity enabled precision printing (Fig. 5b) with 84% printability improvement as ink sipped into the canal of the TRX-cells® layer. Due to the canopy effect arising from 15% CaCO3 filler in the commercial A4 paper, the cells were not entirely stuck on the fibres. The "sipping and floating" effect allows sharp prints. Floated ink was the plausible hidden mark on the other leaf of the paper. The phenomena allow ink saving due to the reduction of the dendrite (B1 in Fig. 5a) and micro splash (S in Fig. 5a), sipping of inkjet inks into nano canals in Fig. 5c.

In rice-grain coating with the violet pigment of *Clitorea ternatea*, TRX-cells® acted as pigment immobilizer, chauffeuring the ink to the surface of the grain. Due to the higher pigment-starch affinity, the violet 'rushed' into the core of the grains as soon as contact occurred. Heat treatment after coating left TRX-cells® functioning as a thermo-blanket. Combined with the thermo effect, xylan in TRX-cells® allowed longer grain shelf life given the preservative characteristics of xylan.

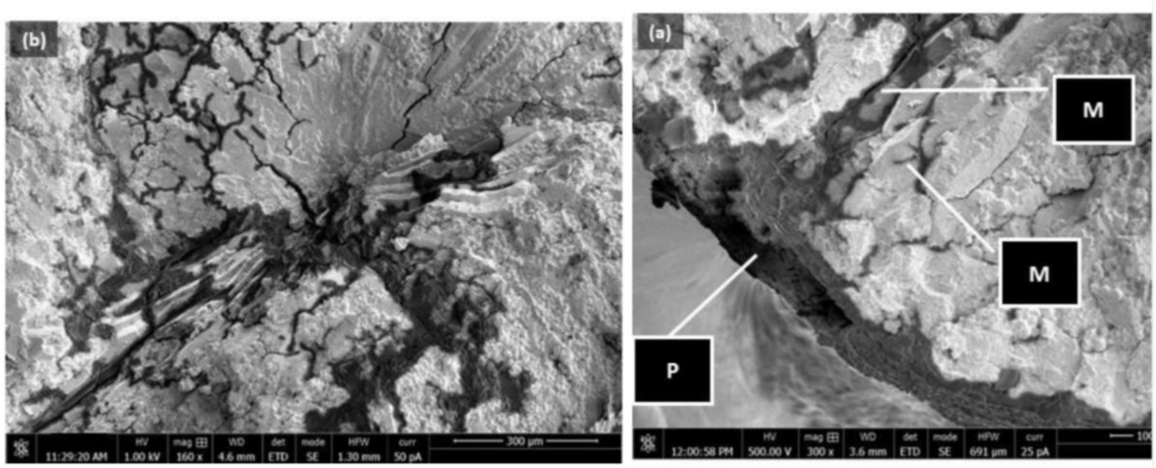


**Figure 6:** Rice grain coated with pigment-loaded TRX-cells®. Reproduced from Ghazali et al., 2021b.

**TRX-cells®: Circular Nanotechnology for Biomass Management:** In the whole research picture, TRX-cells® production is nestled snugly in the circular oil palm residue management model. The circular resource management within TRX production itself is much simpler than the envisioned framework for NFC or bioethanol production from EFB in the prior analyses [28].

The model in Figure 7 also houses the already materialised Thai mushroom production [28] using EFB as a growth substrate. The idea has unlocked EFB as a practical feedstock for bioethanol production post-mushroom harvest for the food and pharmaceutical markets. Such a smart move prepares the feedstock for a renewable energy material and simultaneously minimising waste alongside bioethanol generation and mushrooms for food security. The model also envisions the oil palm industry as the quadruple-edge revenue analogous to the biomass circularity model of the rubber and rubberwood industry [29]. Actualisation of the model would enhance the GDP contribution from the palm oil mill and plantation to the country.

An alternative low-energy process discovered in this study (Process X, Figure 7) is capable of converting both fibres and biomass to nano cells provided fine-tuning is made in the biomass preprocessing stage. Details of this will be discussed elsewhere.

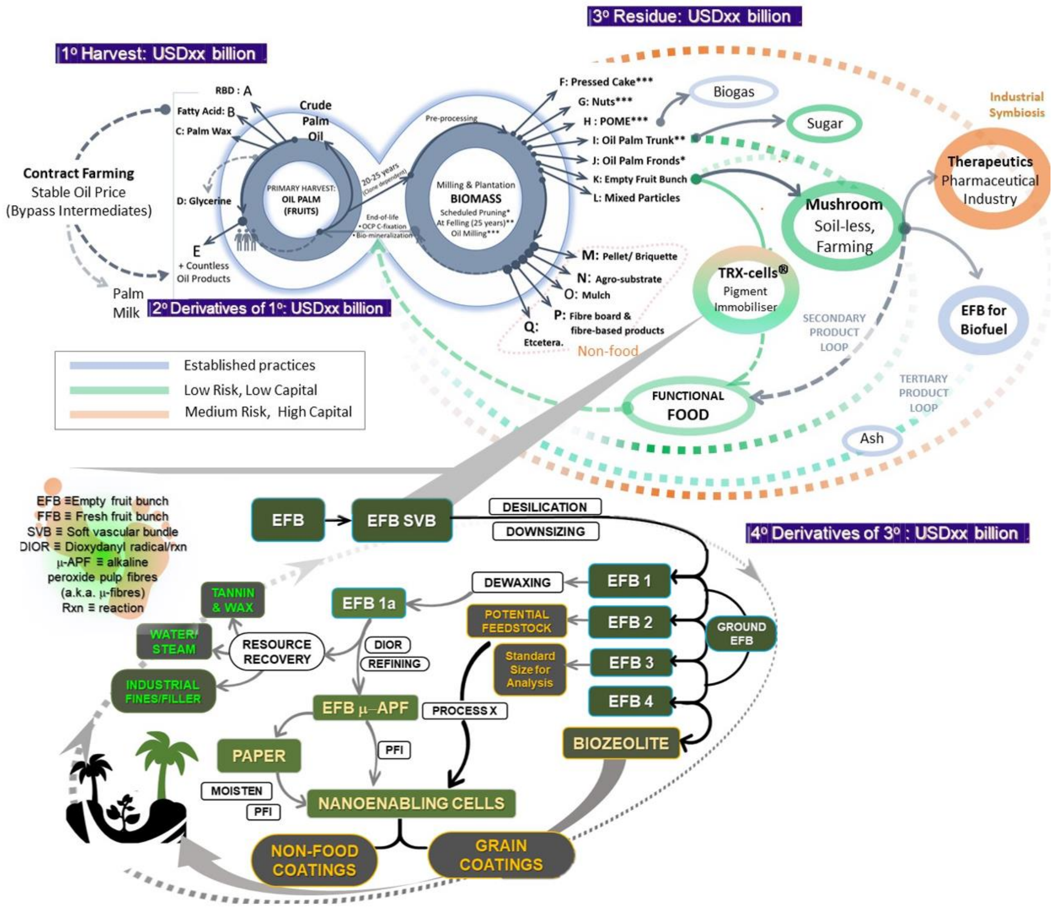


**Figure 7**: Circular nanotechnology for EFB. Reproduced from https://doi.org/10.1016/j.heliyon.2024.e30824.

## 4. CONCLUSION

TRX-cells® ultra-high yield reasoned by the coexistence of cellulose and non-cellulose differentiates it from nanocellulose rods and crystals widely reported in the literature. The unique components of TRX-cells® were the main enablers of its application in precision print and grain coating. The plethora of usable commodities generated along the nano-cell production implies the process' good fit into the circularity model, engendering the desired *closed, extended, and intensifying loops strategy for ultimate carbon sequestration as end-of-life.* The potential NFC-alternative cells generated via rapid process illuminate the nanotechnology venture nestling within the circular oil palm residue (OPR) management. Leveraging the resource-efficient criteria of the DIOR system provides crystal clear directives towards the clear-sighted circular nanotechnology in EFB utilisation not only to prevent waste accumulation and the associated systemic impacts from pest infestation, fouling, open burning and emission but also to generate profits while preparing the material for subsequent. Beyond mechanisms of circular nanotechnology, actualising circularity in oil palm farming and palm oil milling sheds promises to lift the pain plaguing oil palm smallholders. Maximising every opportunity for equity downstream and upstream would create balance for the sustainability and prosperity of the industry.

**ACHIEVEMENT**

i) Publications:

- **Ghazali, A.**, Azhar, N. H., Mohd Salleh, R., Khairuddean, M., Rafatullah, L. & Mahmud SH, (2024) Nano Cells from Fruit Bunch Residue: Nestling Nanotechnology within the Circular Oil Palm Milling Residue Management, Heliyon, 10 e30824 (2024) https://doi.org/10.1016/j.heliyon.2024.e30824 [WoS Q1 IF3.4]
- **Ghazali, A.**, Azhar, N. H., Mohd Salleh, R., Khairuddean, M., Rafatullah, L. & Mahmud SH, (2024) Supplementary Materials to Nano Cells from Fruit Bunch Residue: Nestling Nanotechnology within the Circular Oil Palm Milling Residue Management, Heliyon, 10 e30824 (2024). https://www.cell.com/cms/10.1016/j.heliyon.2024.e30824/attachment/eec12673-1423-4d3f-a8c2-3d1bb837ad3a/mmc1.pdf [WoS Q1 IF3.4]
- **Ghazali, A.**, N Azhar, Mahmud SH, Khairudin MF, Ahmad I, Rafatullah M, Zaini MA, Yusof Y. (2021) Delaminated cells for nano-enabled inkjet printability. Cellulose Chemistry and Technology, 55, 9–10, 1071–1081. [WoS Q2; IF1.288]
- **Ghazali, A.**, Mohd Salleh, R., Ahmad, M. Q., Azhar, N. and Malik, M. F. A. (2021). Capturing Anthocyanin Immobilization On Rice Through The Ultra-High Resolution Electron Lenses. Malaysian Journal of Microscopy, 17(2):20-31. (18) (PDF) CAPTURING ANTHOCYANIN IMMOBILIZATION ON RICE THROUGH THE ULTRA-HIGH RESOLUTION ELECTRON LENSES (researchgate.net) [SCOPUS Q4]
- **Ghazali, A.** & Azhar, N. H. (2023). Inscribing the Compositional Changes of Heterogeneous Bio-system through FTIR Spectroscopy – Demonstration of Guideline to Sound Interpretation. Journal of Advanced Research in Applied Sciences and Engineering Technology 29, Issue 2 (2023) 276-290. https://doi.org/10.37934/araset.29.2.276290
- **Ghazali, A.** "Reconceptualizing Industrial By-Products: Biomass Circularity for People and Nature". Bioremediation Technologies: For Wastewater and Sustainable Circular Bioeconomy, edited by Riti Thapar Kapoor and Mohd Rafatullah, Berlin, Boston: De Gruyter, 2023, pp. 23-56. https://doi.org/10.1515/9783111016825-002 [WoS]
- **Ghazali, A.** & Nik Haikal. (in press) 'Soil Revitalization – Biochar Engendering Circular Biomass Management for Climate Mitigation', in Catalytic Applications of Biochar for Environmental Remediation, American Chemical Society, ACS, Ritti Kapoor, Rafatullah Lari, Silanpaa (eds). [WoS/SCOPUS]

**Ghazali, A. ≡ Arniza Ghazali**

ii) **Human Capital Development**

The project leader screened for a master student to pursue the first-year milestones in a staggered manner throughout Covid-19 lockdown and the new norms. Several final year students also successfully graduated between 2021 to 2023 applying seed ideas from the research.

iii) **Intellectual Property**

– Trademark Registration in Malaysia:

No. **TM2021001302** TM "TRX-cells" in Class 01 In the name of UNIVERSITI SAINS MALAYSIA.

| **Copyright Title** | *File Number* |
|---|---|
| XP-LOGIC FRAMEWORK FOR PADDY PROCESSING | CRLY2023P06808 |
| CIRCULAR BIOECONOMY MODEL FOR RUBBER AND RUBBERWOOD AS NON-FOOD BIOMASS | CRLY2023P06802 |
| XP-LOGIC FRAMEWORK FOR RUBBERWOOD RESIDUES | CRLY2023P06803 |
| MODEL BIOEKONOMI KITARAN BAGI GETAH DAN KAYU GETAH DENGAN SIMBIOSIS INDUSTRI | CRLY2023P06804 |
| GENERAL CIRCULAR BIOECONOMY MODEL FOR AGROCOMMODITY | CRLY2023P06805 |
| MAP OF POWERFUL BUSINESS MODELS - GUIDE TO VARIOUS PROFIT CHAINS | CRLY2023P06806` |
| XP-LOGIC FRAMEWORK FOR OIL PALM RESIDUES | CRLY2023P06807 |

## REFERENCES


[1] A. Ghazali, W. D. Wanrosli, K. N. Law, Alkaline peroxide mechanical pulping of oil palm lignocellulosics: Part 2-EFB responses to pretreatments, Appita Journal, 59 (1) (2006), 65- 70.

[2] C. J. Cort, W. L. Bohn, Alkaline Peroxide Mechanical Pulping of hardwoods. TAPPI Journal 74 (6) (1991), 79.

[3] H. Bukhart, B. Pelech, D. I. H. Munster, New BCTMP grades for quality improvement and cost reduction of paper machine furnishes, Proceedings of the 54th Annual Convention of ATIP, France (2001), (pp. 9-11).

[4] E. C. Xu, APMP pulps from non-wood fibres. Part 1: Kenaf and straw, Appita Journal 54 (5) (2001), 444-448.

[5] Y. M. Dermawan, A. Ghazali, W. D. Wanrosli, Effect of multiple impregnation on APP of EFB, Cellulose Chemistry and Technology 45 (5-6) (2011), 355-360.

[6] N. H. Kamaluddin, A. Ghazali, W. D. Wan Rosli, Potential of fines as reinforcing fibres in APP of OP EFB, BioResources 7 (3) (2012), 3425-3438.

[7] C. Pena, B. Civit, Gallego, A. Schmid, A. Druckman, A. Caldeira- Pires, B. Weidema, E. Mieras, F. Wang, J. Fava, I. Milà i Canals, M. Cordella, P. Arbuckle, S. Valdivia, S. Fallaha, W. Motta, Using Life Cycle Assessment to achieve a circular economy. Life Cycle Initiative (2020), https://pure.manchester.ac.uk/ws/files/175169708/Pena_et_al_2020_Using_LCA_to_achieve_circular_economy_LCI_July_2020.pdf, Accessed December 12, 2023.

[8] R. Yusoff, A. N. Azizul, (2022, February 7), Towards a sustainable paper consumption and printing practices, https://news.iium.edu.my/?p=162372, Accessed December 4. 2023.

[9] A. Ghazali, N. H. Azhar, S. Mahmud, M. F. Khairudin, I. Ahmad, M. Rafatullah, M. A. Zaini, Y. Yusof, Delaminated cells for nano-enabled inkjet printability. Cellulose Chemistry and Technology, 55 (9-10) (2021a) 1071–1081.

[10] M. E. Morales, S. Lhuillery, M. Ghobakhloo, Circularity Effect in the Viability of Bio-Based Industrial Symbiosis: Tackling extraordinary events in value chains. Journal of Cleaner Production, 348 (2022) 131387, https://doi.org/10.1016/j.jclepro.2022.131387

[11] A. Ferrer, I. Filpponen, A. Rodríguez, J. Laine, O. J. Rojas, Valorization of residual Empty Palm Fruit Bunch Fibers (EPFBF) by microfluidization: production of nanofibrillated cellulose and EPFBF nanopaper. Bioresource Technology, 125 (2012), 249-255.

[12] A. Ghazali, M. R. H. Mohd Zukeri, W. D. Wanrosli, B. Azahari, R. Ibrahim, T. Ahmed, I. Rushdan, A. K. Ziya, Augmentation of EFB fibre web by nano-scale fibrous elements. Advanced Materials Research, 832 (2014a), 494-499.

[13] S. Paavilainen, T. Rog, I. Vattulainen, Analysis of twisting of cellulose nanofibrils in atomic molecular dynamics simulations, The Journal of Physical Chemistry B, 115 (14) (2011), 3747-3755.

[14] M. Wohlert, T. Benselfelt, L. Wagberg, I. Furo, L. A. Berglund, J. Wohlert, Cellulose and the role of hydrogen bonding: not in charge of everything, Cellulose, 29 (2022), 1-23. https://doi.org/10.1007/s10570-021-04325-4

[15] Technical Association of Pulp and Paper Industry, TAPPI, (1997), T414 om-98 Elmendorf Tear Resistance of Paper, TAPPI Standard test methods, TAPPI Press.

[16] Technical Association of Pulp and Paper Industry, TAPPI, (1997), T425 Opacity, TAPPI Standard test methods, TAPPI Press.

[17] S. Park, J. O. Baker, M. E. Himmel, P. A. Parilla, D. K. Johnson, Cellulose crystallinity index: measurement techniques and their impact on interpreting cellulase performance, Biotechnology for Biofuels, 3 (2010) 1-10

[18] D. Ciolacu, F. Ciolacu, V. Popa, Amorphous cellulose: structure and characterization. Cellulose Chemistry and Technology, 45 (1-2) (2010), 13-21.

[19] B. Zhang, S. B. Hutchens, On the relationship between cutting and tearing in soft elastic solids, Soft Matter, 17 (28) (2021) 6728-6741, https://doi.org/10.1039/D1SM00527H.

[20] K. Bircher, M. Zündel, M. Pensalfini, A. E. Ehret, E. Mazza, Tear resistance of soft collagenous tissues, Nature communications 10 (1) (2019) 792, https://doi.org/10.1038/s41467-019-08723-y

[21] Morris, B. A. (2017). Plastics Design Library, The Science and Technology of Flexible Packaging. In Barry A. Morris (Eds.) Strength, stiffness, and abuse resistance (pp. 309-350). Elsevier (2017) https://doi.org/10.1016/B978-0-323-24273-8.00009-5

[22] A. Miletzky, M. Punz, H. Weber, P. Wollboldt, R. Krasser, W. Bauer, R. Schennach, Improvement of paper strength by increasing the xylan content. Advances in pulp and paper research, Cambridge (2013) 887-906.

[23] E. Eltahan, Structural parameters affecting tear strength of fabrics tents, Alexandria Engineering Journal, 57 (2018) 97-105, https://doi.org/10.1016/j.aej.2016.12.005

[29] A. Ghazali, M. Zbiec, Rich dad and poor dad: Biomass circularity sciences empathizing rubber smallholders, Journal of Advanced Research in Applied Science and Engineering Technology, 29 (1) (2022) 207–222, https://doi.org/10.37934/araset.29.1.207222

[25] C. Thulluri, R. Balasubramaniam, H. R. Velankar, Generation of highly amenable cellulose-Iβ via selective delignification of rice straw using a reusable cyclic ether-assisted deep eutectic solvent system, Scientific Report, 11 (2021) 1591, https://doi.org/10.1038/s41598-020-80719-x

[26] D. Ye, S. Rongpipi, S. N. Kiemle, W. J. Barnes, A. M. Chaves, C. Zhu, ... E. D. Gomez, Preferred crystallographic orientation of cellulose in plant primary cell walls, Nature communications 11 (1) (2020) 4720.

[27] M. S. Zamil, A. Geitmann, The middle lamella—more than a glue. Physical Biology, 14 (1) (2017) 015004, https://doi.org/10.1088/1478-3975/aa5ba5

[28] C. Mamimin, S. Chanthong, C, Leamdum, S. O-Thong, P. Prasertsan, Improvement of empty palm fruit bunches; biodegradability and biogas production by integrating the straw mushroom cultivation as a pretreatment in the solid-state anaerobic digestion, Bioresource Technology 319 (2021), 124227

**APPENDIX – Talent Development**
**Master Candidate's International Conference Presentation**

## Objectives:

- Improves OPB-inkjet compatibility ←
- Identifies surface engineering agent (SEA) to supplement / alternative filler - of non-fossil origin.
- Defines mechanism and function: filler, coat or extender? ←
- Project local benefits. ←




## Printability Terminology & Calculation

- Coverage:
  - [(Printed grid) /Printed Grid for Commercial A4] x 100
- Stray: Dots that do not land on the programmed region ("off-grid dots", OGD)
- Bleed: spread of ink within the specified 1° and 2° regions.

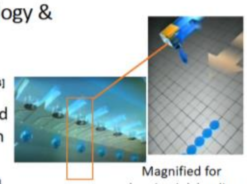

Magnified for showing ink landing as dots & precise distribution.



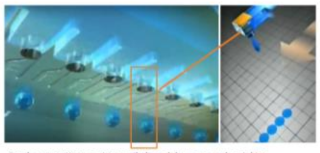

Pembesaran: Konsep titisan pikoliter dalam percetakan inkjet.





## Methodology




## Results – paper charges improved – thus toner coverage: 53.90% for (a) and 82.17% for (b).

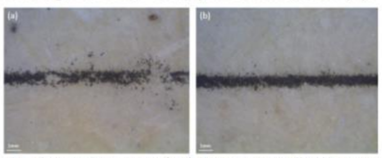


Laser prints of a pressed coarse paper (PCP) showing coverage offered by toner continuity (a) without and (b) with coatings.



## Results – masking by functional nanocells improved porosity.

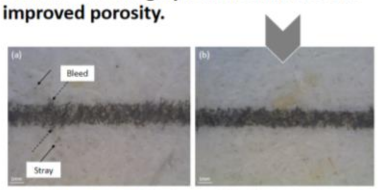


Bleed on OPB paper from EFB (a) without and (b) with functional nanocell coat.



## Results – Benchmark print: stray is rare on inkjet prints

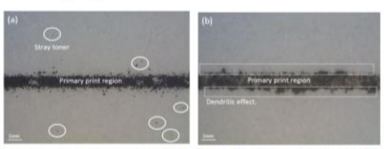


Print outcome for **commercial A4** with (a) stray toner particles on laser jet print and (b) **bleed** manifesting as the dendritic effect arising from **fluid capillary motion in inkjet print.**



## Results – functional cells improved surface affinity for inkjet prints

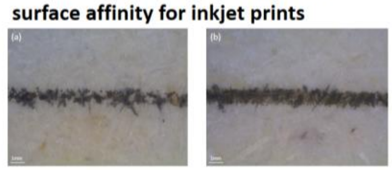


Inkjet prints of a metal-pressed coarse paper (PCP) showing inkjet coverage (a) without and (b) with coatings.



## Masking

- Filling effect was fulfilled by nanofibrill creeping into the inter-fibre gaps.
- Masking or micro-pores – when nanocells landed on the surface of the gap.
- Canopy – only observed on commercial A4 due to the presence of $CaCO_3$. The partial covering resulting in canopy had hidden the inorganic fillers and improved the surface affinity for inkjet fluid.

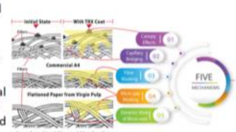






## Conclusion

- Functional cells delaminated from the non-recyclable microfibres from EFB **serves the surface engineering purpose**.
- Nanocells gave **predominantly masking** rather than filling – ∴ a complementary additive to $CaCO_3$.
- Certain surface improved laserjet prints – depending of aqueous media & cells effects on the surface's initial state.
- **Commercial A4 more compatible with inkjet & other problematic surfaces.**
- Multifunctionality achieved: Besides Pinacell™, potential application in packaging industry where inkjet printing will be prominent.

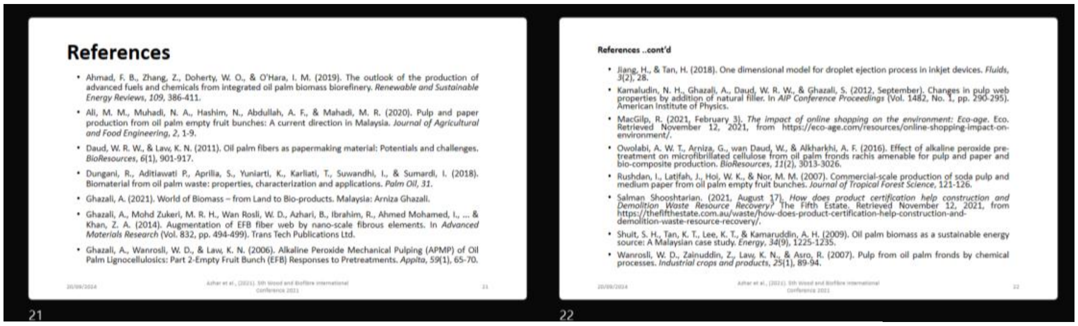


## References

- Ahmad, F. B., Zhang, Z., Doherty, W. O., & O'Hara, I. M. (2019). The outlook of the production of advanced fuels and chemicals from integrated oil palm biomass biorefinery. *Renewable and Sustainable Energy Reviews, 109*, 386-411.
- Ali, M. M., Muhadi, N. A., Hashim, N., Abdullah, A. F., & Mahadi, M. R. (2020). Pulp and paper production from oil palm empty fruit bunches: A current direction in Malaysia. *Journal of Agricultural and Food Engineering, 2*, 1-9.
- Daud, W. R. W., & Law, K. N. (2011). Oil palm fibers as papermaking material: Potentials and challenges. *BioResources, 6*(1), 901-917.
- Dungani, R., Aditiawati P., Aprilia, S., Yuniarti, K., Karliati, T., Suwandhi, I., & Sumardi, I. (2018). Biomaterial from oil palm waste: properties, characterization and applications. *Palm Oil, 31*.
- Ghazali, A. (2021). World of Biomass – from Land to Bio-products. Malaysia: Arniza Ghazali.
- Ghazali, A., Mohd Zukeri, M. R. H., Wan Rosli, W. D., Azhari, B., Ibrahim, R., Ahmed Mohamed, I., ... & Khan, Z. A. (2014). Augmentation of EFB fiber web by nano-scale fibrous elements. In *Advanced Materials Research* (Vol. 832, pp. 494-499). Trans Tech Publications Ltd.
- Ghazali, A., Wanrosli, W. D., & Law, K. N. (2006). Alkaline Peroxide Mechanical Pulping (APMP) of Oil Palm Lignocellulosics: Part 2-Empty Fruit Bunch (EFB) Responses to Pretreatments. *Appita*, 59(1), 65-70.

21

**References ..cont'd**

- Jiang, H., & Tan, H. (2018). One dimensional model for droplet ejection process in inkjet devices. *Fluids*, 3(2), 28.
- Kamaludin, N. H., Ghazali, A., Daud, W. R. W., & Ghazali, S. (2012, September). Changes in pulp web properties by addition of natural filler. In *AIP Conference Proceedings* (Vol. 1482, No. 1, pp. 290-295). American Institute of Physics.
- MacGilp, R. (2021, February 3). *The impact of online shopping on the environment: Eco-age*. Eco. Retrieved November 12, 2021, from https://eco-age.com/resources/online-shopping-impact-on-environment/.
- Owolabi, A. W. T., Arniza, G., wan Daud, W., & Alkharkhi, A. F. (2016). Effect of alkaline peroxide pre-treatment on microfibrillated cellulose from oil palm fronds rachis amenable for pulp and paper and bio-composite production. *BioResources, 11*(2), 3013-3026.
- Rushdan, I., Latifah, J., Hoi, W. K., & Nor, M. M. (2007). Commercial-scale production of soda pulp and medium paper from oil palm empty fruit bunches. *Journal of Tropical Forest Science*, 121-126.
- Salman Shooshtarian. (2021, August 17). *How does product certification help construction and Demolition Waste Resource Recovery?* The Fifth Estate. Retrieved November 12, 2021, from https://thefifthestate.com.au/waste/how-does-product-certification-help-construction-and-demolition-waste-resource-recovery/.
- Shuit, S. H., Tan, K. T., Lee, K. T., & Kamaruddin, A. H. (2009). Oil palm biomass as a sustainable energy source: A Malaysian case study. *Energy, 34*(9), 1225-1235.
- Wanrosli, W. D., Zainuddin, Z., Law, K. N., & Asro, R. (2007). Pulp from oil palm fronds by chemical processes. *Industrial crops and products, 25*(1), 89-94.

22



# Acknowledgement

The project was executed with funding from the Ministry of Higher Education (MOHE) FRGS/1/2019/STG07/USM/02/8 in realizing the Sustainable Development Goal, SDG 3 (Good Health and Well-being) and SDG 12, Responsible Consumption & Production.




---

## DISCLAIMER

This write-up condenses the findings of the long research to 15 pages. The comprehensive details on theEFB fibre deconstruction to TRX-cells® are in Heliyon accessible at https://doi.org/10.1016/j.heliyon.2024.e30824 and https://www.cell.com/cms/10.1016/j.heliyon.2024.e30824/attachment/eec12673-1423-4d3f-a8c2-3d1bb837ad3a/mmc1.pdf Details on applications are in https://doi.org/10.35812/cellulosechemtechnol.2021.55.92 and **Malaysian Journal of Microscopy,** 17(2):20-31. (18) (PDF) CAPTURING ANTHOCYANIN IMMOBILIZATION ON RICE THROUGH THE ULTRA-HIGH RESOLUTION ELECTRON LENSES (researchgate.net)